ACS POLYMERS Au
AN OPEN ACCESS JOURNAL OF THE AMERICAN CHEMICAL SOCIETY

pubs.acs.org/polymerau

Article

Quantification of Water–Ion Pair Interactions in Polyelectrolyte Multilayers Using a Quartz Crystal Microbalance Method

Chikaodinaka I. Eneh, Tuuva Kastinen, Suyash Oka, Piotr Batys, Maria Sammalkorpi, and Jodie L. Lutkenhaus*

Cite This: *ACS Polym. Au* 2022, 2, 287–298

Read Online

ACCESS | Metrics & More | Article Recommendations | Supporting Information

ABSTRACT: Water existing within thin polyelectrolyte multilayer (PEM) films has significant influence on their physical, chemical, and thermal properties, having implications for applications including energy storage, smart coatings, and biomedical systems. Ionic strength, salt type, and terminating layer are known to influence PEM swelling. However, knowledge of water's microenvironment within a PEM, whether that water is affiliated with intrinsic or extrinsic ion pairs, remains lacking. Here, we examine the influence of both assembly and post-assembly conditions on the water–ion pair interactions of poly(styrene sulfonate)/poly(diallyldimethylammonium) (PSS/PDADMA) PEMs in NaCl and KBr. This is accomplished by developing a methodology in which quartz crystal microbalance with dissipation monitoring is applied to estimate the number of water molecules affiliated with an ion pair (i), as well as the hydration coefficient, $\pi_{salt}^{H_2O}$. PSS/PDADMA PEMs are assembled in varying ionic strengths of either NaCl and KBr and then exposed post-assembly to increasing ionic strengths of matching salt type. A linear relationship between the total amount of water per intrinsic ion pair and the post-assembly salt concentration was obtained at post-assembly salt concentrations >0.5 M, yielding estimates for both i and $\pi_{salt}^{H_2O}$. We observe higher values of i and $\pi_{salt}^{H_2O}$ in KBr-assembled PEMs due to KBr being more effective in doping the assembly because of KBr's more chaotropic nature as compared to NaCl. Lastly, when PSS is the terminating layer, i decreases in value due to PSS's hydrophobic nature. Classical and *ab initio* molecular dynamics provide a microstructural view as to how NaCl and KBr interact with individual polyelectrolytes and the involved water shells. Put together, this study provides further insight into the understanding of existing water microenvironments in PEMs and the effects of both assembly and post-assembly conditions.

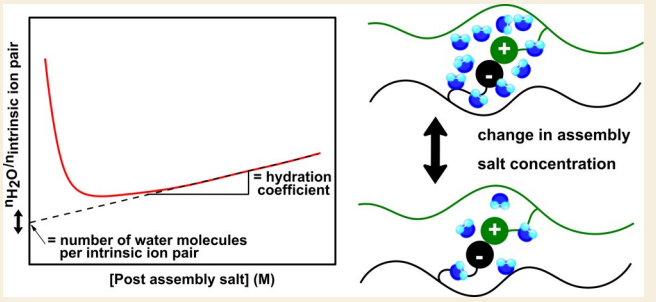

KEYWORDS: *polyelectrolyte multilayers, swelling, quartz crystal microbalance with dissipation, layer-by-layer assembly, intrinsic ion pairs, salts, doping*

INTRODUCTION

Polyelectrolyte complexes (PECs) prepared into thin films are called polyelectrolyte multilayers (PEMs).[1−4] Assembly occurs when polycations and polyanions form intrinsic ion pairs, leaving other uncompensated charge sites available for extrinsic ion compensation by smaller counterions.[1,5,6] These PEMs may be applied in electrochemical systems, drug delivery platforms, smart coatings, and water and gas barriers.[7−11] They are highly tunable and responsive to changes in assembly conditions (*e.g.*, polymer concentration, salt type and concentration, pH, and temperature) and also post-assembly environment (*e.g.*, temperature, humidity, and ionic strength).[4,12−16] Thus, to ensure the integrity of a PEM in its final application, it is important to understand its stability from assembly to end use in response to external stimuli.

PECs and PEMs have been described as "saloplastics" due to the strong plasticizing effect of salt, which reduces the number of intrinsic ion pairs among polyelectrolyte chains.[17,18] This is often described as doping.[19,20] The effects of increasing salt content on a macroscopic level are evident in PEM growth profiles (linear to exponential growth), mechanical properties (rigid to soft), layer structure (stratified to interdigitated layers), surface roughness (rough to smooth), and glass transition temperature (T_g).[18,21−24] Interestingly, post-assembly exposure of the PEM to salt may either result in swelling, deswelling, or even disassembly of the PEM depending on the ionic strength.[25−27]

Similar to salt, water acts as a plasticizer in PEMs by increasing the free volume for polymer mobility and weakening electrostatic attraction between oppositely charged polyelectrolytes.[28,29] Our past studies have shown a universal

Received: March 5, 2022
Revised: April 6, 2022
Accepted: April 7, 2022
Published: April 21, 2022

dependence of key PEM properties, such as glass transition temperature (T_g) and relaxation time (τ), on water content for both strong and weak polyelectrolytes at varying pH and ionic strength.[16,22,30] Specifically, the inverse of T_g was proportional to the ratio of total water molecules to total number of intrinsic ion pairs,[22,30] pointing to the significance of water's association with the polycation−polyanion intrinsic ion pair.

A number of studies classify the total water content in PEMs into smaller microenvironments.[22,31−33] In our recent work, by observing the hydrogen bonding strengths of the deconvoluted OD stretch peak obtained for poly(styrene sulfonate)/poly(diallyldimethylammonium) (PSS/PDADMA) PEMs using attenuated total reflectance Fourier transform infrared (ATR-FTIR) spectroscopy, we identified three water microenvironments around ion pairs: high frequency (tightly bound) water, low frequency (loosely bound) water, and bulk (free) water.[31] A prominent finding from the study is the lack of any bulk free water for both partially and fully immersed PEMs, indicating that all water molecules present in the PEMs are associated with and influenced by either intrinsic or extrinsic ion pairs.[31] Although the nature of the water microenvironment was examined, the study could not distinguish whether water was located at extrinsic or intrinsic ion pairs.

Experimentally, the Schlenoff group developed a method to distinguish between intrinsic and extrinsic water−ion pair interactions using ATR-FTIR spectroscopy.[27] Two polycations, PDADMA, and poly(4-vinylmethylpyridinium bromide) (P4VMP) were assembled with PSS at 1.0 M NaCl, annealed in 1.0 M NaCl for a week, and then exposed to varying concentrations of a range of 14 different salts. The purpose of the annealing step was to produce PEMs with a 1:1 polycation:polyanion stoichiometric ratio. The number of total water molecules per intrinsic ion pair, r_{H_2O}, was determined from the areas of the OH and SO_3^- peaks and plotted against the post-assembly salt concentration. By extrapolating the linear portion of the resulting curve to the y-axis, the number of water molecules associated with intrinsic ion pairs for an undoped PEM, "i", was determined by the intercept and a hydration coefficient, $\pi_{salt}^{H_2O}$, determined by the slope. $\pi_{salt}^{H_2O}$ represents the ability of a salt to influence an influx of water into a PEM. For PSS/PDADMA or PSS/P4VMP PEMs, the values of i were 6.9 ± 1.7 or 2.5 ± 0.6 water molecules per intrinsic ion pair, respectively, showing that P4VMP is a more hydrophobic polycation. It was observed that i remains constant irrespective of the post-assembly salt whereas $\pi_{salt}^{H_2O}$ is dependent on the post-assembly salt type. This study serves as motivation to broaden the available methodology to determine i and the factors influencing i. In our case, we employ quartz crystal microbalance with dissipation (QCM-D) monitoring, which provides a method to directly measure mass changes with both assembly and post-assembly conditions, leading to an alternative method to assess water at the intrinsic ion pairs.

QCM-D over the years has become a relevant tool for studying the response of polymers and composites to changes in external environment. QCM-D, which operates on the converse-piezoelectric effect of quartz crystal, serves as an effective way to measure real-time changes in PEM thickness, mass, and viscoelasticity.[34,35] From our group, past works of Reid *et al.* involved the study of the reversible swelling behavior of PSS/PDADMA PEMs prepared at 0.5 M NaCl upon post-assembly exposure to different concentrations of varying divalent salt solutions.[36] Also, O'Neal *et al.* studied the swelling−deswelling behavior and the compositional changes of PSS/PDADMA PEMs prepared at 0.5 M NaCl upon exposure to different concentrations of monovalent salts (KBr, NaBr, NaCl, and KCl).[25] None of these studies quantitatively examined the water content or the water's microenvironment with regard to intrinsic or extrinsic ion pairs.

In this study, we estimate the number of water molecules associated with intrinsic ion pairs in PSS/PDADMA PEMs prepared in NaCl and KBr using QCM-D. We monitor both the layer-by-layer (LbL) assembly and the post-assembly swelling or deswelling in solutions of different salt concentrations in real time. Molecular dynamics (MD) simulations provide a microscopic viewpoint of water at the intrinsic pair. The goal is to develop a method by which QCM-D can estimate the number of water molecules affiliated with an ion pair, as well as the hydration coefficient, i and $\pi_{salt}^{H_2O}$, respectively. Once obtained, we discuss how i and $\pi_{salt}^{H_2O}$ are influenced by salt identity and the PEM's terminating layer.

EXPERIMENTAL SECTION

Materials

Poly(diallyldimethylammonium) (PDADMA, M_w = 200,000−350,000 g/mol, 20 wt % solution), poly(styrene sulfonate) (PSS, M_w = 500,000 g/mol), and linear polyethylenimine (LPEI, M_w = 25,000 g/mol) were purchased from Sigma-Aldrich, Scientific Polymer Products, and Polysciences, Inc., respectively. Sodium chloride (NaCl) and potassium bromide (KBr) were purchased from Sigma-Aldrich and Alfa Aesar, respectively. Silicon dioxide-coated QSensors (QSX 303 SiO_2) QCM-D substrates were purchased from Biolin Scientific.

Preparation of Freestanding Polyelectrolyte Multilayers (PEMs)

An automated Carl Zeiss HMS slide stainer was used to fabricate freestanding PSS/PDADMA PEMs on Teflon substrates. First, PDADMA and PSS solutions were prepared at 1 g/L concentration and at identical NaCl or KBr ionic strength. The ionic strength for each salt was varied from 0.25−1.0 M (0.25, 0.5, 0.75, and 1.0 M). Eight samples of PSS/PDADMA PEMs were prepared: four in the presence of NaCl and four in the presence of KBr. The Teflon substrates were sonicated in ethanol for 15 min followed by thorough rinsing with Milli-Q water. The first layer was fabricated by dipping the substrates in PDADMA solution of a certain ionic strength for 15 min, followed by three separate rinse steps for 2, 1, and 1 min in Milli-Q water at matching ionic strength. The same process was repeated for the second layer by replacing the PDADMA solution with a PSS solution to form a layer pair. A total of 140 layer pairs were prepared with a final rinse step in pure Milli-Q water for 5 s to remove any excess salt. The PEMs were dried under ambient conditions overnight and then dried under vacuum at 115 °C for 3 h. The completed PEMs are denoted as $(PSS/PDADMA)_{140}$.

Quartz Crystal Microbalance with Dissipation (QCM-D) Monitoring

Quartz crystal microbalance with dissipation (QCM-D) monitoring was used to monitor both LbL assembly and post-assembly behavior using a QSense E4 instrument. The PEMs were assembled on SiO_2-coated AT-cut quartz crystals with a resonant frequency of 4.95 MHz. The quartz crystals were cleaned by immersing them in 2 vol % sodium dodecyl sulfate (SDS) for 10 min, rinsing with Milli-Q water, drying with nitrogen, and one last step of 15 min O_2-plasma treatment. PDADMA and PSS polyelectrolyte solutions were prepared at a concentration of 0.1 g/L at varying ionic strengths of NaCl and KBr (0.25−1.0 M) similar to that of the freestanding films. Rinse solutions were set at a matching ionic strength to that of the polyelectrolyte solutions. LPEI solution was adjusted to pH 5.5 to

https://doi.org/10.1021/acspolymersau.2c00008
ACS Polym. Au 2022, 2, 287−298

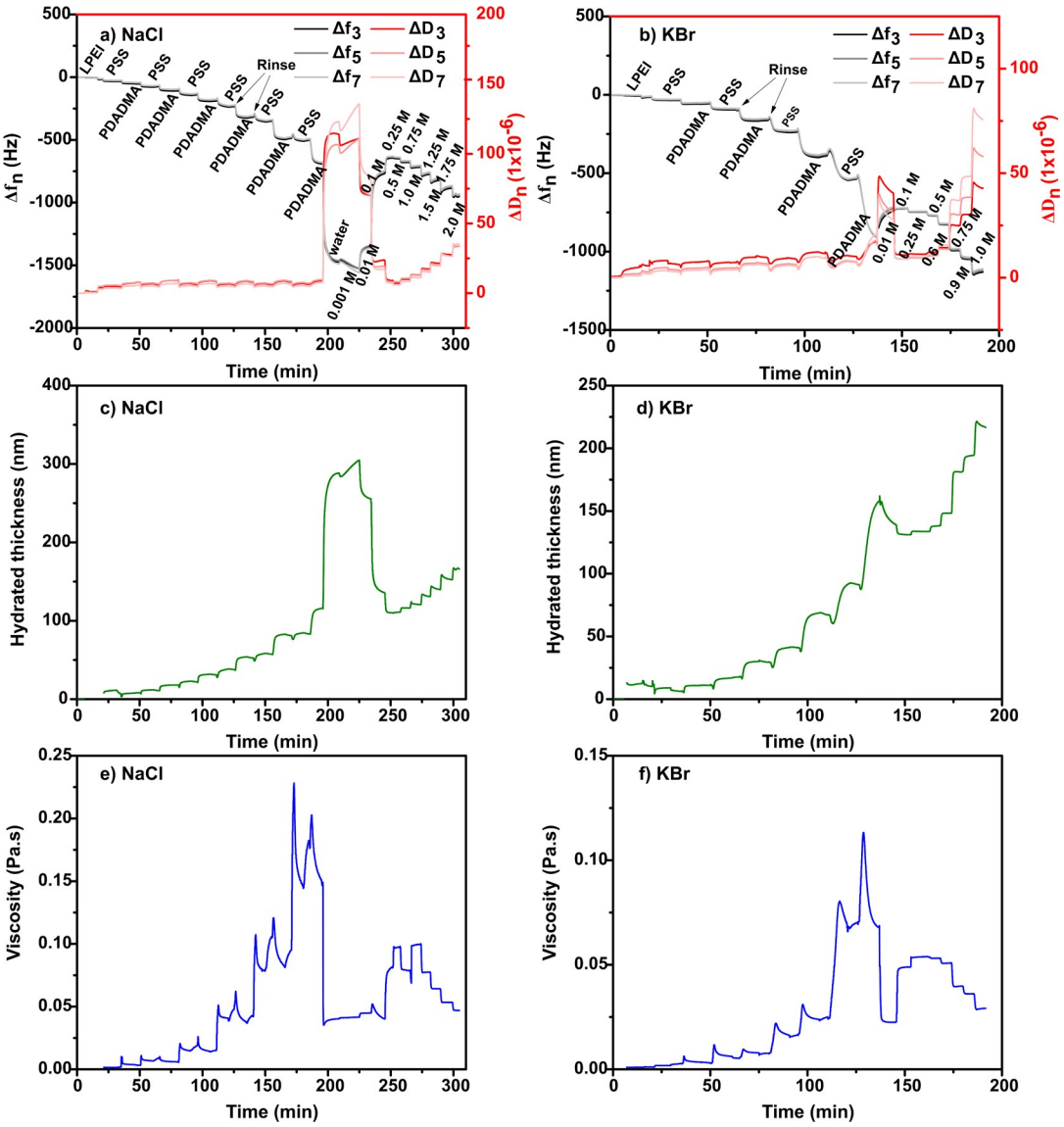

Figure 1. Δf_n and ΔD_n versus time for the 3rd, 5th, and 7th overtones (n) of the QCM-D response from the layer-by-layer deposition and post-assembly salt treatment of (a) $(PSS/PDADMA)_6$ PEMs prepared at 0.5 M NaCl, post-assembly salt treatment in NaCl; (b) $(PSS/PDADMA)_4$ PEMs prepared at 0.5 M KBr, post-assembly salt treatment in KBr. (c,d) Resulting hydrated thickness (e,f) and viscosity from viscoelastic modeling of the QCM-D response in (a) and (b), respectively.

obtain a stable clear solution. All QCM-D experiments were carried out at room temperature. All polyelectrolyte and rinse solutions were flowed through a peristaltic pump at a constant approximate flowrate of 150 μL/min. Milli-Q water (pH 5.5) was first allowed to flow over the quartz crystal for 30 min as a baseline for each measurement. An anchor layer of LPEI was then deposited onto the crystal for 10 min before rinsing for 5 min with pure Milli-Q water. The rest of the LbL film followed an alternating deposition of PSS and PDADMA solutions for 10 min each separated by a 5 min rinse at a matching ionic strength.

The final number of layers is designated "x" in $(PSS/PDADMA)_x$. For PEMs prepared in NaCl, $x = 6$, and for those prepared in KBr, $x = 4$ in order for the film thicknesses to stay within the QCM-D operational limits.[34] This is because the QCM-D guide suggests that this thickness limit exists at approximately 1 μm, beyond which overtone signals begin to become unstable, starting with the highest overtone (13th overtone).[34,35] In order to accurately model the resulting QCM-D data for a viscoelastic film, a minimum of 3 overtones are required. We, therefore, aimed to have all PEM thicknesses below 700 nm during both assembly and post-assembly experiments. Also, some PEMs were terminated with either PDADMA for $(PSS/PDADMA)_{x\,=\,4\text{ or }6}$ or PSS for $(PSS/PDADMA)_{x\,=\,4.5\text{ or }6.5}$.

Post-assembly, PEMs were exposed to solutions of increasing salt concentrations (0−2.0 M for NaCl and 0−1.0 M for KBr) with an exposure time of 30 min for each salt. The low salt region (0−0.1 M) was in some cases eliminated if the corresponding swelling thickness went beyond the permissible thickness range. In such cases, the lowest salt concentration explored were 0.001 M NaCl and 0.1 M KBr. At the end of all QCM-D measurements, each sample was rinsed in pure Milli-Q water to remove any excess salt on the crystal.

Determining the Salt Hydration Coefficient, $\pi_{salt}^{H_2O}$, and the Number of Water Molecules Associated with Intrinsic Ion Pairs, i

From the raw QCM-D data, the hydrated thickness of the PEM was calculated using a viscoelastic model under each exposure condition. The PEMs were then dried, and the dry thickness of the film was measured using profilometry (see the SI). Using the reported density of dry PSS/PDADMA PEMs (ρ_{dry} = 1.27 kg/m^3), the dry mass of the PEMs was calculated from its dry thickness.[20,37] The water content of the PEM at a given state was obtained by subtracting the dry PEM

https://doi.org/10.1021/acspolymersau.2c00008
ACS Polym. Au 2022, 2, 287−298

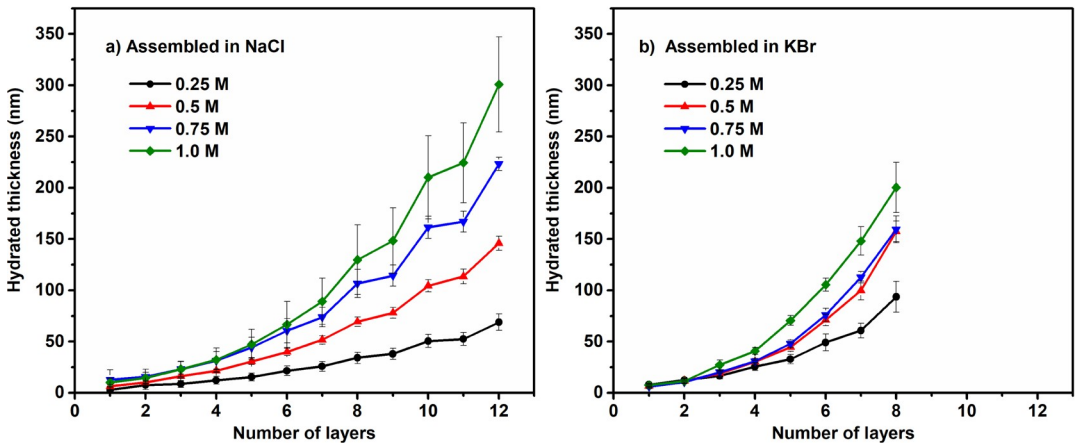

Figure 2. Growth profiles of PSS/PDADMA PEMs assembled in (a) NaCl and (b) KBr at varying concentrations. Hydrated thicknesses were obtained from viscoelastic modeling of QCM-D data, such as those shown in Figure 1. All experiments were repeated three times, and the error bars represent the standard deviation. Odd layers represent PSS deposition, and even layers represent PDADMA deposition.

mass from the hydrated mass. Dry, freestanding PEMs were made separately, and a representative composition was obtained using NMR spectroscopy and XPS (see the SI). Assuming that all of the limiting polyelectrolyte in each sample engages in intrinsic charge compensation only, r_{H_2O} was estimated from the composition and the PEM's water content. The combination of all the experimental procedures outlined above makes it possible to directly estimate the hydration coefficient, $\pi_{salt}^{H_2O}$, and the number of water molecules associated with intrinsic ion pairs in an undoped complex, *i*. Ref 27 provides a derivation toward these two parameters. $\pi_{salt}^{H_2O}$ is defined by the equation below:

$$\pi_{salt}^{H_2O} = \frac{r_{H_2O} - i}{[MA_n]} \quad (1)$$

$$r_{H_2O} = \frac{n_{H_2O}}{n_{PSS}} \quad (2)$$

where $[MA_n]$ is the salt concentration and r_{H_2O} is the ratio of moles of water in the PEM to moles of PSS monomer units in the PEM. In this study, non-stoichiometric PEMs with PDADMA in excess were prepared; thus, PSS represents the limiting polyelectrolyte in the PEM. We therefore assume that all PSS chains in the PEM form intrinsic ion pairs. By rearranging eq 1, a linear relationship between r_{H_2O} and [MA] is obtained, in which the slope is equal to $\pi_{salt}^{H_2O}$ and in which the *y* intercept is equal to *i*:

$$r_{H_2O} = \pi_{salt}^{H_2O}[MA] + i \quad (3)$$

For most polyelectrolyte systems studied, a deviation from this linear relationship between r_{H_2O} and [MA] is observed at lower salt concentrations (<0.1 M) due to electrostatic repulsion within the PEMs causing increased swelling. Another explanation is that this may occur as a result of osmotic pressure, which brings in additional water into the multilayer films at low salt concentrations. Therefore, only the linear portion of the curve (existing at higher salt concentrations) was extrapolated to the *y* axis to determine both *i* and $\pi_{salt}^{H_2O}$.

Simulation Methodology

The simulation protocol and methodology for both MD and *ab initio* molecular dynamics (AIMD) simulations are detailed in the Supporting Information.

RESULTS

Layer-by Layer-Assembly

QCM-D was applied to monitor the growth and the swelling responses of the $(PSS/PDADMA)_x$ PEMs in real time. First, a layer of LPEI at pH 5.5 was deposited onto a bare SiO_2-coated QCM-D sensor to promote subsequent layer growth. Following this, LbL assembly of PSS and PDADMA was conducted at varying NaCl or KBr concentrations (0, 0.25, 0.5, 0.75, 1.0 M). After assembly, the PEM was exposed to solutions of successively higher salt concentrations and the swelling response was examined. Figure 1 shows examples of the raw data obtained from this procedure for $(PSS/PDADMA)_x$ PEMs prepared at 0.5 M NaCl (Figure 1a) and 0.5 M KBr (Figure 1b) that were then exposed to solutions of NaCl (0−2 M) and KBr (0−1 M), respectively. Generally, a negative frequency change ($\Delta f < 0$) corresponds to an increase in hydrated mass and thickness, and a positive dissipation change ($\Delta D > 0$) corresponds to a softening of the film. In Figure 1, we observed negative changes in frequency with each polyelectrolyte deposition step, confirming an increase in film thickness. For the PDADMA adsorption step, specifically, we observed a more prominent decrease in frequency relative to the PSS step. Rinsing showed small, but noticeable, positive deviations in frequency that we associate with the removal of loosely bound material. At the later stages of film growth, a larger drop in frequency with PDADMA deposition resulted, pointing to an exponential growth trend; for PSS deposition at later stages, frequency did not change much, also consistent with prior reports of exponential growth.[4,24,38−41] Other assembly salt concentrations explored herein generally followed the same responses shown in Figure 1 but to varying magnitudes. The post-assembly swelling responses of the PEMs to solutions of varying salt concentrations and types will be discussed later below.

Figure 1c−f shows the resulting modeled film thickness and viscosity. We observed that the film viscosity increased with film thickness as more polymer layers were adsorbed during assembly. Hence, during assembly, each deposition step caused an increase in the amount of adsorbed and hydrated polymer, leading to an increase in the viscous component of the PEM. However, during post-assembly monitoring, when exposed to pure water, an influx of water molecules causes swelling and reduced the viscosity. Likewise, with the introduction of salt ions to the PEMs post-assembly, as the PEMs either swelled or deswelled, the viscosity either decreased or increased, respectively.

https://doi.org/10.1021/acspolymersau.2c00008
ACS Polym. Au 2022, 2, 287−298

Figure 2 shows the growth profile of the PSS/PDADMA PEMs extracted from data similar to that shown in Figure 1. For all samples prepared, we observed a linear growth regime at early stages, after which a non-linear exponential (or parabolic) growth regime manifested. This growth trend mirrors the large frequency drops that were observed upon the deposition of PDADMA at later stages, Figure 1a,b. Comparing Figure 2a to 2b, it becomes clear that PEMs assembled in KBr have a thickness larger than those assembled in NaCl for an equivalent number of layers. Quantitatively, for $x = 4$ layer pairs (8 layers) and an assembly salt concentration of 1.0 M, the average hydrated film thickness was 130 nm for NaCl-assembled PEMs and 200 nm for KBr-assembled PEMs. For comparison, Figure S1 shows the final dry thickness of PEMs measured using profilometry for each of the assembly conditions, in which the final dry thickness increased as the assembly salt concentration increased.

Taken together, these growth profiles show the influence of salt concentration and salt type on the growth mechanism and growth rate of a PEM. From Figure 2a,b, it is evident that increasing salt concentration leads to thicker layer pairs, consistent with previous studies.[4,42−44] This is because salt screens the charges on the polyelectrolytes, weakening their interactions and changing their conformation from an extended chain to a more coil-like conformation.[23,42,45,46] As for the salt type, NaCl-assembled PSS/PDADMA PEMs grew more slowly than the KBr-assembled ones, Figure 2. This is because NaCl is more kosmotropic than KBr, so NaCl is less effective at extrinsic charge compensation, leading to the lower growth rate.[4,47] This has previously been reported by experiments and simulations alike, in which the more hydrated ions (Na^+, Cl^-) generally bind more weakly to the polyelectrolyte charge sites.[45] Similar results have been identified for complex doping with NaCl and KBr.[19,48]

Composition of PSS/PDADMA PEMs Assembled at Various NaCl and KBr Concentrations

Because we desire to understand the swelling response of the PEM on a molecular level, it is important to identify the PEM's composition. Thus, two measurement techniques were applied to calculate the PDADMA and PSS compositions: ^{1}H NMR spectroscopy and X-ray photon spectroscopy (XPS).

First, ^{1}H NMR spectroscopy was performed on freestanding $(PSS/PDADMA)_{140}$ PEMs at each studied assembly salt concentration following the same procedure as past studies from our group,[22,25] Table 1 and Figure S2. For PEMs assembled at all concentrations of NaCl, the molar percentage of PSS in the PEM ranged from 43.8 to 45.5%. Similarly, for PEMs assembled from KBr, the molar percentage of PSS was 35.7 to 45.8%. For the assembly salt concentrations studied here (0−1 M), we generally observed no significant influence on the film's composition. Our past investigation of PEMs assembled in only 0.5 M NaCl or KBr yielded a similar percentage of PSS.[49]

Table 1. PDADMA and PSS Composition from ^{1}H NMR Spectroscopy of Freestanding $(PSS/PDADMA)_{140}$ PEMs Prepared at Varying Concentrations of NaCl and KBr

assembly salt	assembly salt concentration (M)	PSS/PDADMA	PSS mol %	PDADMA mol %
NaCl	0.25	0.8	45.5	54.5
	0.5	0.8	44.1	55.9
	0.75	0.8	44.1	55.9
	1.0	0.8	43.8	56.3
KBr	0.25	0.6	36.8	63.3
	0.5	0.6	39.2	60.9
	0.75	0.6	35.7	64.3
	1.0	0.8	45.8	54.2

The NMR results above were taken from PEMs comprising 140 layer pairs, which is quite different from the PEMs comprising 4−6 layer pairs used in QCM-D measurements. To examine PEM composition for the samples used in QCM-D, XPS was performed. The areas of the high-resolution peaks of sulfur (S) in PSS and nitrogen (N) in PDADMA were computed relative to the high-resolution peak of carbon (C), shown in Figure S3. XPS results presented in Table S2 give a PSS percentage of 39.9 to 58.4% for NaCl-assembled PEMs and 44.8 to 62.6% for KBr-assembled PEMs. Table S2 shows two data outliers, which we attribute to experimental error or the limited penetration depth of the XPS method.

Overall, despite the large difference in the number of layer pairs and the method of preparation, both NMR spectroscopy and XPS techniques resulted in relatively similar compositions for the PEMs. Early studies on the growth regimes of the PEMs suggest that PEMs at later growth stages such as these at 140-layer pairs (for NMR spectroscopy) exist in the exponential growth regime in which polyelectrolyte chains exist in a more intertwined state. However, the PEMs made at $x = 4$ or 6 (for XPS and QCM-D) are formed in earlier growth stages such that the PEMs are still influenced by the individual polyelectrolyte chains and interactions with the substrate. Given these considerations, we used the results obtained from ^{1}H NMR spectroscopy for our further analysis to remain consistent with our previous works.

It is notable that PDADMA is the majority component in the PEMs. This indicates that most (or all) of the PSS is occupied in intrinsic ion pairing and that PDADMA participates in both intrinsic and extrinsic ion pairs. The presence of excess PDADMA is further confirmed through examination of the raw QCM-D data shown in Figure 1a,b, where each PDADMA deposition step led to a greater frequency decrease than the following PSS deposition step. While complexes and multilayers with a 1:1 stoichiometric have been obtained using an extra annealing step,[50,51] many reports show a non-stoichiometric composition of PSS/PDADMA PEMs similar to observations herein.[4,17,52]

Post-Assembly Swelling Response

As earlier described, PSS/PDADMA PEMs were exposed to increasing concentrations of salt matching the assembly salt type, either NaCl (0−2.0 M) or KBr (0−1.0 M). These concentration ranges were chosen taking into consideration the critical salt concentration for PSS/PDADMA complexes in NaCl (∼2.0 M) and KBr (∼1.6 M) as well as the QCM-D thickness limit.[26,53,54] Figure 3 presents the hydrated thickness at each post-assembly salt concentration obtained from an extended viscoelastic model applied to the QCM-D data. In general, as the assembly salt concentration increases, the hydrated thickness increases. Specifically, PEMs assembled at 1.0 M NaCl and KBr (green triangles) both exhibited hydrated thicknesses greater than those assembled at 0.25 M (black squares), regardless of post-assembly salt exposure. This is consistent with the growth profiles shown in Figure 2. By observation, three major swelling regions are observed for the range of post-assembly salt conditions, indicated by the

https://doi.org/10.1021/acspolymersau.2c00008
ACS Polym. Au 2022, 2, 287−298

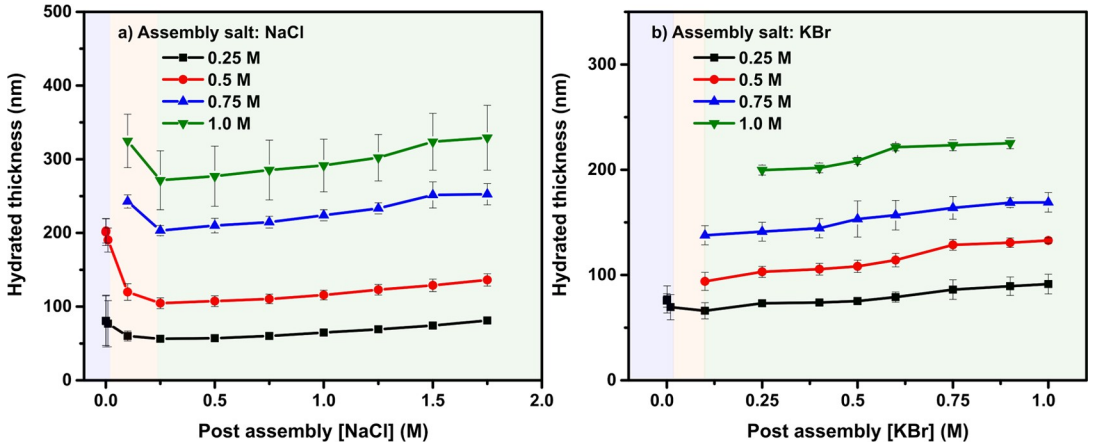

Figure 3. Hydrated thickness of (a) $(PSS/PDADMA)_6$ PEMs assembled in NaCl and (b) $(PSS/PDADMA)_4$ PEMs assembled in KBr at each post-assembly salt concentration. Blue shading represents the zero to low salt concentration region; orange represents the intermediate salt concentration region; and green represents the mid to high salt concentration region for both NaCl and KBr post-assembly exposures.

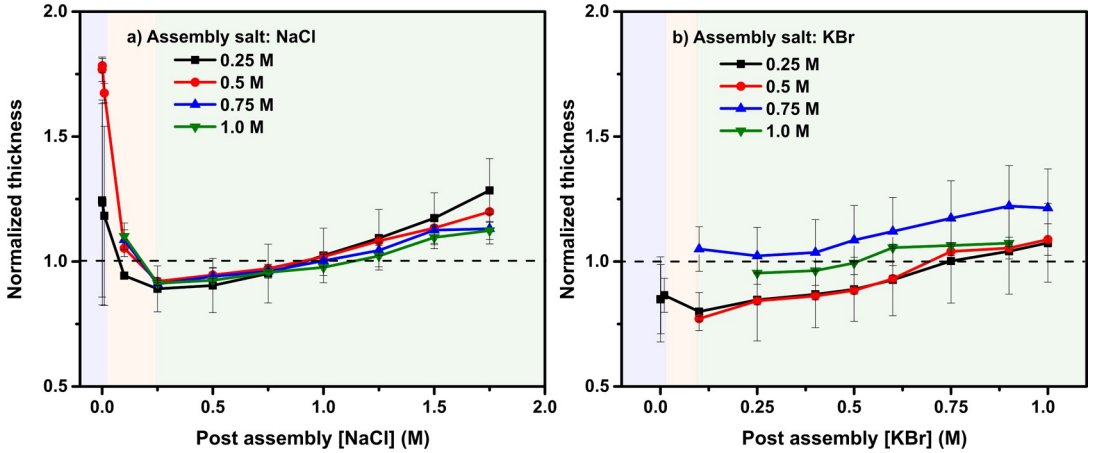

Figure 4. Post-assembly swelling thickness normalized to the final assembly thickness of (a) $(PSS/PDADMA)_6$ assembled in NaCl and (b) $(PSS/PDADMA)_4$ assembled in KBr. Specifically, the final assembly thickness is that of the PEM freshly prepared at the assembly salt concentration indicated but before the PEM's exposure to media of varying salt concentrations.

different shaded regions. These swelling regions have been observed elsewhere in experimental and simulation studies of doping, swelling, and ion-pairing properties.[25,27,31,45,55]

In the first region (blue), at low post-assembly salt concentrations (0−0.1 M NaCl and 0−0.01 M KBr), the PEM experiences a large influx of water and counterions − so much so that several samples (assembled at>0.75 M NaCl and >0.5 M KBr) swelled beyond the range of our QCM-D instrument's measurement range. Recalling that PDADMA exists in excess within the PEM, the film swells to allow for charge compensation of uncompensated extrinsic PDADMA sites at low salt concentrations of the contacting solution.[22,25] However, charge compensation is restricted due to the larger Debye screening length, leading to a small fraction of PDADMA units that are not ion-paired.[25] This results in electrostatic self-repulsion and significant swelling.

In the second region (orange), at intermediate salt concentrations (0.1−0.25 M NaCl and 0.01−0.1 M KBr), a slight deswelling of the PEM is observed. This can be attributed to the sufficient charge screening provided by the salt counterions, causing the PEMs to become more closely packed with less free volume for water. As more salt is added to the PEM from the contacting solution, the previously uncompensated chains become compensated, and electrostatic self-repulsion is minimized.

In the last region (green), at high salt concentrations (0.25−2.0 M NaCl and 0.1−1.0 M KBr), the PEMs begin to swell again. In this case, the swelling results from excess counterions, leading to the formation of additional extrinsic sites. This region exhibits a linear trend of the hydrated thickness with the post-assembly salt concentration. This process by which intrinsic ion pairs are broken to form extrinsic ion pairs due to the introduction of salt ions into the PEMs is also known as doping. The amount of doping and the overall amount of salt in a complex follows a Hofmeister series, in which more hydrophobic salt ions are better dopants.[20] The tendency of a salt to break intrinsic ion pairs is given by the doping constant K_{unpair}:

$$K_{unpair} = \frac{y^2[PE]_{PEC}}{(1-y)[salt]^2} \quad (4)$$

where y is the fraction of intrinsic ion pairs broken or the doping level, $[PE]_{PEC}$ is the concentration of polyelectrolyte in complex, and [salt] is the NaCl or KBr salt concentration.

In Figure 4, we present the post-assembly hydrated thicknesses of the PEMs normalized against the hydrated

https://doi.org/10.1021/acspolymersau.2c00008
ACS Polym. Au 2022, 2, 287−298

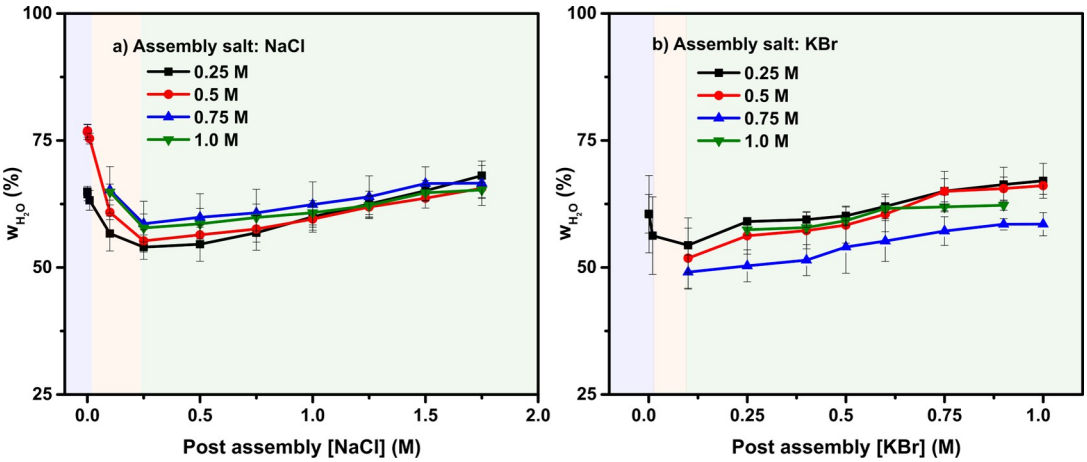

Figure 5. Percentage of water by mass (w_{H_2O}) in (a) $(PSS/PDADMA)_6$ PEMs assembled in NaCl and (b) $(PSS/PDADMA)_4$ assembled in KBr.

thicknesses of those freshly prepared at the assembly salt concentration indicated. This data represents a normalization of the hydrated thickness in Figure 3 to that of their original hydrated states. In the first swelling region (blue), the normalized thickness increased with the assembly salt concentration. Specifically for post-assembly exposure to 0 M salt concentration (Figure 4a), the normalized thickness for PEMs assembled in 0.25 M NaCl was 1.25 ± 0.39, and for those assembled in 0.5 M NaCl, the normalized thickness was 1.77 ± 0.05. In line with our expectations, a 4-layer pair PSS/PDADMA PEM prepared in 1.0 M NaCl doubled in thickness when exposed to water at 0 M salt concentration.[55] Taken together, this shows an increase in the swelling of the PEM due to an influx of water. In the second swelling region (orange), the normalized thickness drops below 1.0, suggesting that the film shrinks beyond its initial hydrated thickness. Here, we observe that all the NaCl assembly concentrations overlap to a similar degree. Last, in the third swelling region (green), we observe a steady increase in normalized thickness with increasing post-assembly salt. The behavior for PEMs assembled from and exposed to KBr (Figure 4b) followed a similar trend to that for NaCl but with some slight differences. Data for the first swelling region is harder to interpret due to a high degree of swelling beyond the instrument's limits. Also, the large error bars allow for only a qualitatively interpretation of the effects of the assembly salt on the post-assembly swelling of KBr.

Similar observations have been made from our past QCM-D studies of PSS/PDADMA PEMs prepared at only at a singular assembly condition of 0.5 M NaCl.[25,36] From the data displayed in Figures 3 and 4, we now discuss the effect of varying assembly conditions (salt type: NaCl and KBr, salt concentration: 0.25−1.0 M) on the post-assembly swelling behavior. Whereas Figure 3 shows an increase in hydrated thickness with increasing assembly salt concentration, Figure 4 shows that actual swelling is independent of the assembly salt concentration. The overlapping of the normalized thickness plots across all salt concentrations points to a general swelling behavior of PSS/PDADMA PEMs in NaCl and KBr. Therefore, we conclude that the swelling in PSS/PDADMA PEMs appear to be "general", regardless of the ionic strength of the assembly salt.

Water Content

We next isolated the percentage of water in the PEM by mass, w_{H_2O}. This calculation requires knowledge of the total PEM mass and thickness in dry and hydrated states (obtained from Figure 3). We obtained the dry PEM thickness from profilometry of multilayers dried after the completion of QCM-D experiments, Figure S1. The water content, w_{H_2O}, was calculated using the density values of PSS/PDADMA PEMs in the dry and hydrated states (ρ_{dry} = 1270 kg/m^3 and $\rho_{hydrated}$ = 1050 kg/m^3, from refs 37 and 25, respectively) to yield Figure 5.

In Figure 5, we observe that w_{H_2O} follows a trend consistent with the three swelling regions described above. This clarifies that the changes in thickness observed are not solely driven by changes in polymer conformation but also the influx of water into the PEMs. Prior to post-assembly salt exposure, w_{H_2O} for all PEMs assembled in NaCl was 53 ± 3% and for those assembled in KBr, it was 59 ± 6%. When exposed to pure water, w_{H_2O} was 58.4 ± 1.3% and 72.3 ± 1.8% for PEMs assembled in 0.25 M and 0.5 M NaCl, respectively. With the increase in ionic strength of the exposure solution, w_{H_2O} dropped to its lowest value of 45% at 0.25 M NaCl post-assembly concentration. Above this, w_{H_2O} increased with increasing post-assembly salt concentration. For the PEMs assembled in 0.25 M KBr, a similar trend was observed, but for lower KBr concentrations, the PEMs swelled outside of the instrument's acceptable parameters (data not shown).

The amount of water in a PEM is influenced by the molecular weight, charge density, and packing density of the polyelectrolyte, as well as the contacting solution's salt type and concentration.[56] Using neutron reflectometry to measure changes in thickness, Hariri *et al.* observed a water content of 80% in PSS/PDADMA complexes prepared in 2.5 M NaCl after exposure to pure water.[57] Elsewhere for PSS/PDADMA PEMs, FTIR spectroscopy was used to observe the ratio of the OH stretch peak to the SO_3^- peak against post-assembly salt concentration. Specifically, the trend in the OH/SO_3^- ratio followed a trend with post-assembly salt similar to that displayed in Figure 5a.[27] This supports the conclusion that the PEM swelling observed herein is a consequence of water and salt.

https://doi.org/10.1021/acspolymersau.2c00008
ACS Polym. Au 2022, 2, 287−298

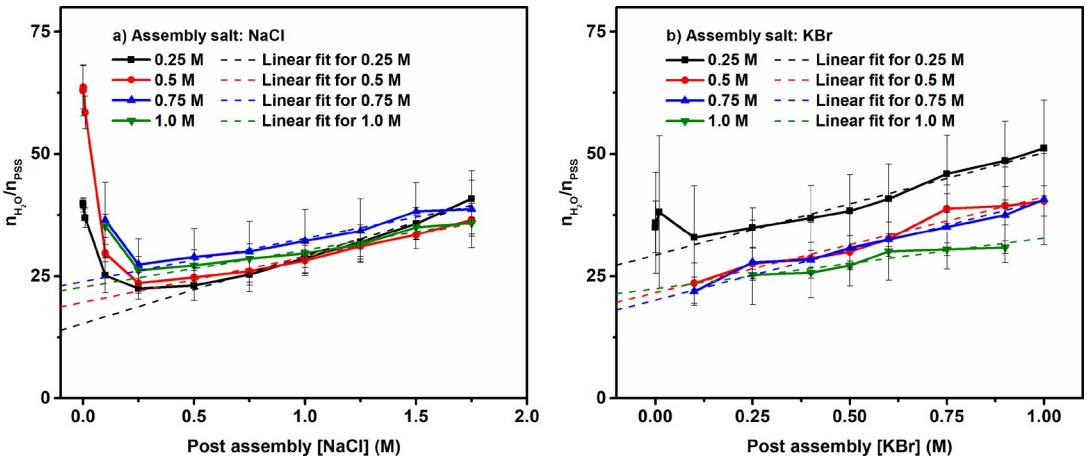

Figure 6. Ratio of total moles of water to moles of PSS repeat units plotted against post-assembly salt concentrations for (a) $(PSS/PDADMA)_6$ assembled in NaCl and (b) $(PSS/PDADMA)_4$ assembled in KBr. The dashed lines show linear fits to the higher-salt regions; the slope is taken as $\pi_{salt}^{H_2O}$, and the y intercept is taken as i.

The PEMs herein are swollen with water, but the exact microenvironment of each water molecule remains undescribed. The molecular distribution of total water content in a PEC or PEM has been captured by various methods based on porosity, water diffusion, neutron reflectometry scattering length density, spectroscopic properties, and thermal characteristics.[22,31,33,58] Large pores have been identified in PSS/PDADMA PEMs using pulse field gradient (PFG) NMR spectroscopy.[58] Many studies have categorized the total water content in a PEM as either pore water or free water.[58,59] In other works, similarly described water states were named void and swelling water using neutron reflectometry.[14,33,60] Through the deconvolution of the OD stretch peak obtained using FTIR spectroscopy of fully immersed PSS/PDADMA PEMs, three water states based on binding energy have been identified.[31] Also, using differential scanning calorimetry (DSC), three water states were identified based on the freezing temperature of PSS/PDADMA and PAH/PAA complexes at varying hydrations.[22,32,61] While these works are aimed at separating bulk water into various water microenvironments within the PEMs, these works do not directly identify whether water molecules are associated with intrinsic or extrinsic sites.

Water Associated with Intrinsic Ion Pairs, i, and Hydration Coefficient, $\pi_{salt}^{H_2O}$

Figure 6 shows a plot of the ratio of the total amount of water present in the PEMs at each post-assembly salt concentration to the amount of PSS repeat units, n_{H_2O}/n_{PSS} or r_{H_2O}. PSS is used here as a representation of the amount of intrinsic ion sites present in the PEM because PSS is the limiting component. By plotting this ratio against the post-assembly salt concentration, we obtain a curve with a high (n_{H_2O}/n_{PSS}) ratio (~60−25) at low salt concentrations and a linear portion at mid to high salt concentrations. The slope of the linear portion is of particular interest because it can be used to estimate the $\pi_{salt}^{H_2O}$, which is defined by eq 3 and describes the doping power of a salt for a specific PEM, as well as how much water a particular salt ion would bring into a PEM upon exposure.

From the hydration coefficients calculated here, we observed that regardless of the assembly salt conditions of the PEMs, there is little influence on the hydration coefficient for KBr and NaCl. PEMs assembled in 0.5−1.0 M NaCl exhibited hydration coefficients of 8.5 ± 0.7 L/mol, and PEMs assembled in 0.25−1.0 M KBr exhibited hydration coefficients of 20.3 ± 1.4 L/mol. Notable exceptions include PEMs assembled at 0.25 M NaCl (13.9 ± 0.9 L/mol) and 1.0 M KBr (10.3 ± 0.9 L/mol). For comparison, Schlenoff *et al.*'s FTIR spectroscopy study yielded a hydration coefficient of 3.8 for a PSS/PDADMA PEM assembled in 1.0 M NaCl with a 1:1 stoichiometry.[27] The difference between the two methods may be attributed to FTIR spectroscopy measuring more strongly bound water and QCM-D measuring both strongly and loosely bound water, or else the different PEM compositions.

Using eq 3 also, the y intercept of the linear portion of the curve in Figure 6 is equal to i, the number of water molecules affiliated with an intrinsic ion pair. i ranges from 15 to 24 water molecules per intrinsic ion pair for NaCl-assembled PEMs, and i ranges from 20 to 29 water molecules per intrinsic ion pair, for KBr-assembled PEMs (Figure S4). Other studies indicate lower values of i. From FTIR spectroscopy, i was 6.9 ± 1.7 for PSS/PDADMA PEMs assembled in 1.0 M NaCl for all post-assembly salts studied.[27] Using neutron reflectivity, the amount of tightly bound, "immobile" water was 3.1 water molecules per PAH/PSS intrinsic ion pair for protonated layers and 1.5 water molecules per monomer pair for deuterated layers.[62] Using NMR spectroscopy, the number of water molecules per ion pair for PSS/PDADMA PEMs exposed to ambient conditions was estimated to be between 5.5 and 7.5 for 3−5 layer pairs.[63] The authors also show that for water-saturated environments, 20−25 water molecules per ion pair are expected.[63] Taken together, i might vary depending on the observation method as well as whether the PEM is immersed or not.

For another viewpoint, we conducted molecular simulations to examine the number of water molecules near PSS and PDADMA charge groups. We observed in MD simulations (non-polarizable, fixed point charge model) that the counter-ion position of Na^+ differs from that of K^+, with Na^+ preferring a location close to a single PSS charge group and K^+ readily shared between two PSS charge groups, at a bridging configuration. The AIMD simulations with polarizable, explicit quantum chemical solvation and ionic group descriptions show a similar tendency for a closer location of Na^+ than that of K^+ for the studied configurations, see Figure 7. In the radial

https://doi.org/10.1021/acspolymersau.2c00008
ACS Polym. Au 2022, 2, 287−298

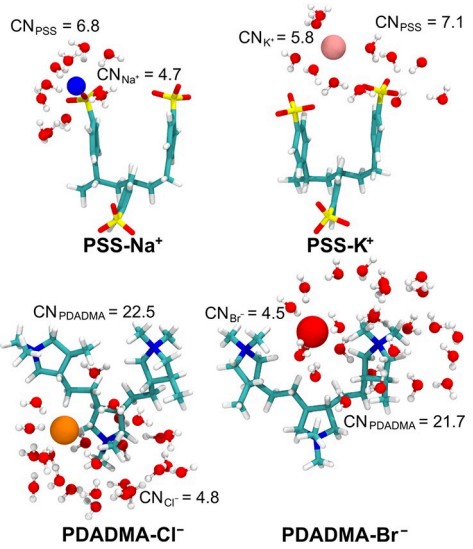

Figure 7. Representative snapshots of the counterion positions around PSS and PDADMA charge groups obtained from the *ab initio* molecular dynamics (AIMD) simulations. A single Na^+, K^+, Cl^-, or Br^- counterion, highlighted in blue, pink, orange, and red, respectively, is present in each system. The coordination numbers (CNs) of the charge group closest to the counterion were calculated between the central atom of the PE charge group (S in PSS and N in PDADMA) and oxygen of water. Similarly, the CNs of the counterions were calculated between the ion and oxygen of water.

distribution function $g(r)$ plot of Figure S5, this manifests as the Na^+ peak maximum being at shorter distance than that of the K^+ counterion. The difference in the counterion location translates to also a binding affinity difference and affects additionally the average distance between the PSS charge groups. These in turn influence PSS conformations and hydration, *e.g.*, coordination number. Additionally, the higher $g(r)$ peak for MD results (Figure S5) suggests stronger binding of Na^+ than K^+ ions to PSS, resulting in a larger number of Na^+ ions condensed around PSS chains, which is in line with the previous studies.[64,65] Considering that at moderate salt concentration, the entropy gain related to the release of counterions is a driving force for complexation, the larger fraction of condensed Na^+ ions can lead to formation of a larger number of intrinsic ion pairs with PDADMA, which was observed experimentally.[49]

The AIMD simulations give also more insight into the solvation of the PE charge groups and counterions. The simulations indicate a notably larger number of water molecules in the first solvation shells of the charge groups of PDADMA (*ca.* 20−23 water molecules) compared to the charge groups of PSS (*ca.* 6−7 water molecules). Although the small system size and short duration of the AIMD simulations cannot reveal this, we would expect counterion specific differences in solvation to influence also the binding distances and PE dynamics. Indeed, when comparing the solvation of the counterions in the PE−ion systems, slightly more water resides around K^+ (*ca.* 6 water molecules) than around Na^+, Cl^-, and Br^- (*ca.* 4−5 water molecules). The K^+ ion also brings a slightly increased amount of water in comparison to Na^+ when binding with the charge groups of PSS. This reflects indirectly in the $g(r)$ peak positions corresponding to PE charge group − counter ion positions of both the MD and AIMD simulations and the peak heights in the MD results (Figure S5).

Based on the water coordination numbers of PSS and PDADMA charge groups, see Figure 7, the number of water molecules around a PSS/PDADMA intrinsic ion pair in a PE assembly can be expected to be slightly smaller than the sum of the water coordination numbers corresponding to PDADMA and PSS separately. This is because of the overlap of their hydration shells when forming an intrinsic ion pair. Considering both the simulations and experimental results here, the number of water molecules around an intrinsic ion pair is expected to be significantly larger than that found, e.g., by Schlenoff *et al.* via FTIR spectroscopy.[27,63] This is because the FTIR and neutron reflectivity method measures only strongly bound water, whereas the QCM-D method likely captures those water molecules both loosely and strongly associated with intrinsic ion pairs.

We next discuss sources of error in our measurements and analysis. First, eq 3 was originally applied to a 1:1 stoichiometric PSS/PDADMA PEM in which the y intercept was taken for a purely undoped PEM with no existing extrinsic ion pairs.[27] However, in our case, the PEMs produced from QCM-D deposition are non-stoichiometric (Table 1 and Table S2). This suggests that our values could be influenced by the presence of extrinsic ion pairs at the condition of no added salt.

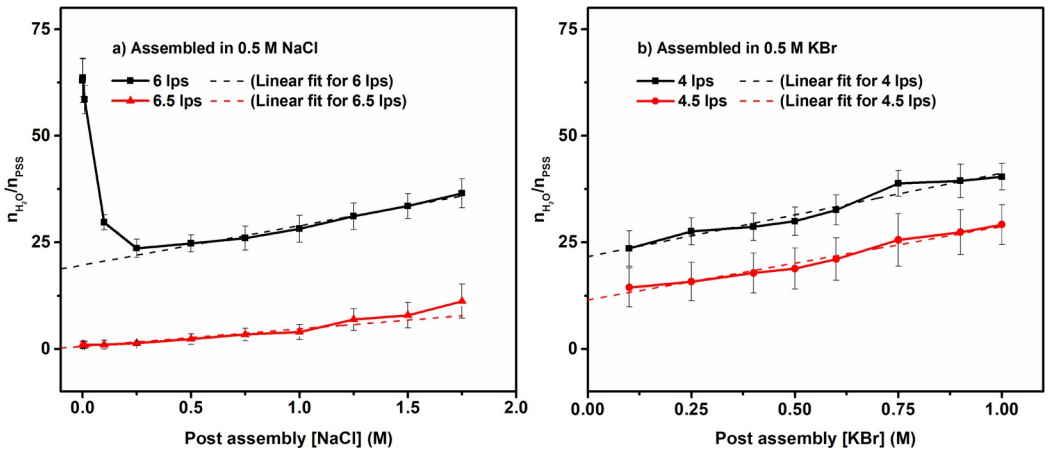

Figure 8. Ratio of total moles of water to intrinsic ion pairs plotted against post-assembly concentrations for (a) $(PSS/PDADMA)_6$ and $(PSS/PDADMA)_{6.5}$ assembled in NaCl and (b) $(PSS/PDADMA)_4$ and $(PSS/PDADMA)_{4.5}$ assembled in KBr.

https://doi.org/10.1021/acspolymersau.2c00008
ACS Polym. Au 2022, 2, 287−298

Second, the assumption that all PSS is in intrinsic ion pairing used in the determination of the amount of intrinsic ion pairs in Figure 6 could also influence the validity of the results as some of the PSS might pair with Cl^-. However, XPS did not reveal the presence of any Cl^-. Third, any errors in the experimental measurement of thickness would also influence the determination of the number of intrinsic ion pairs used in calculation. Last, the density used in QCM-D modeling and calculations would influence the modeled hydrated thickness of the PEM.

Effect of Terminating Layer on $\pi_{salt}^{H_2O}$ and i

PEMs for the preceding results were terminated with PDADMA (x = 4 or 6). In Figure 8, we explore the influence of the terminating layer by assembling PEMs in 0.5 M NaCl and KBr with one extra PSS layer (x = 4.5 or 6.5). Overall, a notable decrease in the water content of the PSS-terminated PEMs is produced. Figure 8a shows a decrease in $\pi_{salt}^{H_2O}$ from 9.25 ± 0.55 to 4.11 ± 0.48 L/mol with an added PSS layer for NaCl. Meanwhile, Figure 8b shows hydration coefficients within error from 19.6 ± 1.9 to 17.3 ± 1.1 L/mol with an added PSS layer for KBr. Also, $\frac{n_{H_2O}}{n_{PSS}}$ for PSS-terminated PEMs was systematically lower than PDADMA-terminated PEMs. Thus, i decreases in value with an added PSS layer, from 19.7 ± 0.6 to 0.63 ± 0.19 and from 21.7 ± 1.2 to 11.5 ± 0.7 moles of water per intrinsic ion pairs with an added PSS layer for NaCl and KBr, respectively.

Many studies have shown the effect of the terminating layer of PEMs on PEM physical and chemical properties. Bruening and Miller demonstrated that PDADMA-terminated or PSS-terminated PEMs in 0.5 M NaCl swelled by 380 ± 60% or 106 ± 9% when immersed in pure water, respectively.[66] This can first be attributed to having hydrophobic PSS existing as the outermost layer of the PEM. The hydrophobicity leads to repulsion of water, evident from the high static water contact angles of ∼70° for PSS-terminated PEMs and ∼20° for PDADMA-terminated PEMs.[67] Also, PDADMA-terminated PEMs exhibit a higher surface anion concentration than PSS-terminated PEMs, which have a net charge of zero.[68,69]

CONCLUSIONS

The response of the water content of PEMs to changes in salt concentration has been extensively studied because of the great impact these changes have on the properties of these multilayer films. In this work, we show the water content responses of PDADMA/PSS PEMs to changes in salt type, salt concentration, and terminating layer. Having understood that water exists in PEMs in various microenvironments, we also further determined both by experiments and simulations the amount of water molecules associated with intrinsic ion pairs, i, in the PEMs and the hydration coefficient, $\pi_{salt}^{H_2O}$, of the salts. Using QCM-D, we identified a fast growth rate and higher post-assembly water content of PEMs assembled in KBr compared to those assembled in NaCl. This is because KBr hydrates PDADMA/PSS PEMs more effectively than NaCl, evident in the significantly higher KBr hydration coefficient. Similarly, NaCl-assembled PEMs exhibited a lower i value when compared to KBr-assembled PEMs at the same ionic strength. MD and AIMD simulations provided support of the closer binding of Na^+ to PSS and pointed toward a difference in counterion position with respect to the PSS charge groups. Both observations affect the solvation of the resulting extrinsic ion pair, and the difference may lead to the formation of less extrinsic sites for the PSS−Na system than for the PSS−K system. This allows for higher influx of water into the PEMs when assembled in KBr. When terminated with the more hydrophobic polyelectrolyte, PSS, both $\pi_{salt}^{H_2O}$ and i were lower than when terminated at PDADMA, proving that the hydrating ability of the salt can also be limited by the exposed polyelectrolyte. We believe that the knowledge provided by this study helps further the understanding of the water−ion pair interactions in complexes.

ASSOCIATED CONTENT

Supporting Information

The Supporting Information is available free of charge at https://pubs.acs.org/doi/10.1021/acspolymersau.2c00008.

QCM-D modeling, proton nuclear magnetic resonance spectroscopy, X-ray photoelectron spectroscopy, profilometry, classical molecular dynamic simulations, and *ab initio* molecular dynamic simulations; plots of "i" and $\pi_{salt}^{H_2O}$ for PSS/PDADMA PEMs prepared at varying concentrations of NaCl and KBr and ion binding radial distribution functions $g(r)$ and corresponding representative snapshots of PSS and PDADMA molecules and the respective ions in the simulations; QTools modeling parameters and XPS-based PEM characterization data (PDF)

AUTHOR INFORMATION

Corresponding Author

Jodie L. Lutkenhaus − *Artie McFerrin Department of Chemical Engineering and Department of Materials Science and Engineering, Texas A&M University, College Station, Texas 77840, United States;* orcid.org/0000-0002-2613-6016; Email: jodie.lutkenhaus@tamu.edu

Authors

Chikaodinaka I. Eneh − *Artie McFerrin Department of Chemical Engineering, Texas A&M University, College Station, Texas 77840, United States*

Tuuva Kastinen − *Department of Chemistry and Materials Science and Academy of Finland Center of Excellence in Life-Inspired Hybrid Materials (LIBER), Aalto University, 00076 Aalto, Finland; Faculty of Engineering and Natural Sciences, Chemistry & Advanced Materials, Tampere University, 33014 Tampere, Finland*

Suyash Oka − *Artie McFerrin Department of Chemical Engineering, Texas A&M University, College Station, Texas 77840, United States*

Piotr Batys − *Jerzy Haber Institute of Catalysis and Surface Chemistry, Polish Academy of Sciences, PL-30239, Krakow 30-239, Poland;* orcid.org/0000-0002-2264-3053

Maria Sammalkorpi − *Department of Chemistry and Materials Science, Academy of Finland Center of Excellence in Life-Inspired Hybrid Materials (LIBER), and Department of Bioproducts and Biosystems, Aalto University, 00076 Aalto, Finland;* orcid.org/0000-0002-9248-430X

Complete contact information is available at: https://pubs.acs.org/10.1021/acspolymersau.2c00008

Author Contributions

The manuscript was written through contributions of all authors. All authors have given approval to the final version of the manuscript.

Funding

This work is supported by the National Science Foundation under Grant No. 1905732, National Science Centre, Poland (Grant No. 2018/31/D/ST5/01866) (P.B.), Academy of Finland Centers of Excellence Program (2022−2029) in Life-Inspired Hybrid Materials (LIBER) under project No. 346111 (M.S.), Academy of Finland project no. 309324 (M.S.), and Finnish Cultural Foundation (T.K.).

Notes

The authors declare no competing financial interest.

■ ACKNOWLEDGMENTS

We thank Rasmus Kronberg and Prof. Kari Laasonen for useful discussions regarding the AIMD modeling. We are grateful for the support by the FinnCERES Materials Bioeconomy Ecosystem. Computational resources by the CSC IT Centre for Science, Finland, RAMI − RawMatTERS Finland Infrastructure, and PLGrid Infrastructure, Poland, are also gratefully acknowledged.

■ REFERENCES

(1) Decher, G.; Hong, J. D.; Schmitt, J. Buildup of ultrathin multilayer films by a self-assembly process: III. Consecutively alternating adsorption of anionic and cationic polyelectrolytes on charged surfaces. *Thin Solid Films* **1992**, *210-211*, 831−835.

(2) Izquierdo, A.; Ono, S. S.; Voegel, J. C.; Schaaf, P.; Decher, G. Dipping versus Spraying: Exploring the Deposition Conditions for Speeding Up Layer-by-Layer Assembly. *Langmuir* **2005**, *21*, 7558−7567.

(3) Lavalle, P.; Gergely, C.; Cuisinier, F. J. G.; Decher, G.; Schaaf, P.; Voegel, J. C.; Picart, C. Comparison of the Structure of Polyelectrolyte Multilayer Films Exhibiting a Linear and an Exponential Growth Regime: An in Situ Atomic Force Microscopy Study. *Macromolecules* **2002**, *35*, 4458−4465.

(4) Ghostine, R. A.; Markarian, M. Z.; Schlenoff, J. B. Asymmetric Growth in Polyelectrolyte Multilayers. *J. Am. Chem. Soc.* **2013**, *135*, 7636−7646.

(5) Meka, V. S.; Sing, M. K. G.; Pichika, M. R.; Nali, S. R.; Kolapalli, V. R. M.; Kesharwani, P. A comprehensive review on polyelectrolyte complexes. *Drug Discovery Today* **2017**, *22*, 1697−1706.

(6) Manoj Lalwani, S.; Eneh, C. I.; Lutkenhaus, J. L. Emerging trends in the dynamics of polyelectrolyte complexes. *Phys. Chem. Chem. Phys.* **2020**, *22*, 24157−24177.

(7) Parveen, N.; Jana, P. K.; Schönhoff, M. Viscoelastic Properties of Polyelectrolyte Multilayers Swollen with Ionic Liquid Solutions. *Polymer* **2019**, *11*, 1285.

(8) Holder, K. M.; Smith, R. J.; Grunlan, J. C. A review of flame retardant nanocoatings prepared using layer-by-layer assembly of polyelectrolytes. *J. Mater. Sci.* **2017**, *52*, 12923−12959.

(9) Suarez-Martinez, P. C.; Robinson, J.; An, H.; Nahas, R. C.; Cinoman, D.; Lutkenhaus, J. L. Polymer-clay nanocomposite coatings as efficient, environment-friendly surface pretreatments for aluminum alloy 2024-T3. *Electrochim. Acta* **2018**, *260*, 73−81.

(10) Lankalapalli, S.; Kolapalli, V. R. M. Polyelectrolyte Complexes: A Review of their Applicability in Drug Delivery Technology. *Indian J. Pharm. Sci.* **2009**, *71*, 481−487.

(11) Li, J.; van Ewijk, G.; van Dijken, D. J.; van der Gucht, J.; de Vos, W. M. Single-Step Application of Polyelectrolyte Complex Films as Oxygen Barrier Coatings. *ACS Appl. Mater. Interfaces* **2021**, *13*, 21844−21853.

(12) Jaber, J. A.; Schlenoff, J. B. Counterions and Water in Polyelectrolyte Multilayers: A Tale of Two Polycations. *Langmuir* **2007**, *23*, 896−901.

(13) Dubas, S. T.; Schlenoff, J. B. Factors Controlling the Growth of Polyelectrolyte Multilayers. *Macromolecules* **1999**, *32*, 8153−8160.

(14) Zerball, M.; Laschewsky, A.; Köhler, R.; Von Klitzing, R. The Effect of Temperature Treatment on the Structure of Polyelectrolyte Multilayers. *Polymer* **2016**, *8*, 120.

(15) vander Straeten, A.; Dupont-Gillain, C. Highly Hydrated Thin Films Obtained via Templating of the Polyelectrolyte Multilayer Internal Structure with Proteins. *ACS Appl. Polym. Mater.* **2020**, *2*, 2602−2611.

(16) Lalwani, S. M.; Batys, P.; Sammalkorpi, M.; Lutkenhaus, J. L. Relaxation Times of Solid-like Polyelectrolyte Complexes of Varying pH and Water Content. *Macromolecules* **2021**, *54*, 7765−7776.

(17) Shamoun, R. F.; Reisch, A.; Schlenoff, J. B. Extruded Saloplastic Polyelectrolyte Complexes. *Adv. Funct. Mater.* **2012**, *22*, 1923−1931.

(18) Porcel, C. H.; Schlenoff, J. B. Compact Polyelectrolyte Complexes: "Saloplastic" Candidates for Biomaterials. *Biomacromolecules* **2009**, *10*, 2968−2975.

(19) Ghostine, R. A.; Shamoun, R. F.; Schlenoff, J. B. Doping and Diffusion in an Extruded Saloplastic Polyelectrolyte Complex. *Macromolecules* **2013**, *46*, 4089−4094.

(20) Yang, M.; Digby, Z. A.; Schlenoff, J. B. Precision Doping of Polyelectrolyte Complexes: Insight on the Role of Ions. *Macromolecules* **2020**, *53*, 5465−5474.

(21) Dodoo, S.; Steitz, R.; Laschewsky, A.; von Klitzing, R. Effect of ionic strength and type of ions on the structure of water swollen polyelectrolyte multilayers. *Phys. Chem. Chem. Phys.* **2011**, *13*, 10318−10325.

(22) Zhang, Y.; Batys, P.; O'Neal, J. T.; Li, F.; Sammalkorpi, M.; Lutkenhaus, J. L. Molecular Origin of the Glass Transition in Polyelectrolyte Assemblies. *ACS Cent. Sci.* **2018**, *4*, 638−644.

(23) McAloney, R. A.; Sinyor, M.; Dudnik, V.; Goh, M. C. Atomic Force Microscopy Studies of Salt Effects on Polyelectrolyte Multilayer Film Morphology. *Langmuir* **2001**, *17*, 6655−6663.

(24) Tang, K.; Besseling, N. A. M. Formation of polyelectrolyte multilayers: ionic strengths and growth regimes. *Soft Matter* **2016**, *12*, 1032−1040.

(25) O'Neal, J. T.; Dai, E. Y.; Zhang, Y.; Clark, K. B.; Wilcox, K. G.; George, I. M.; Ramasamy, N. E.; Enriquez, D.; Batys, P.; Sammalkorpi, M.; Lutkenhaus, J. L. QCM-D Investigation of Swelling Behavior of Layer-by-Layer Thin Films upon Exposure to Monovalent Ions. *Langmuir* **2018**, *34*, 999−1009.

(26) Wang, Q.; Schlenoff, J. B. The Polyelectrolyte Complex/Coacervate Continuum. *Macromolecules* **2014**, *47*, 3108−3116.

(27) Schlenoff, J. B.; Rmaile, A. H.; Bucur, C. B. Hydration Contributions to Association in Polyelectrolyte Multilayers and Complexes: Visualizing Hydrophobicity. *J. Am. Chem. Soc.* **2008**, *130*, 13589−13597.

(28) Zhang, R.; Zhang, Y.; Antila, H. S.; Lutkenhaus, J. L.; Sammalkorpi, M. Role of Salt and Water in the Plasticization of PDAC/PSS Polyelectrolyte Assemblies. *J. Phys. Chem. B* **2017**, *121*, 322−333.

(29) Hodge, R. M.; Bastow, T. J.; Edward, G. H.; Simon, G. P.; Hill, A. J. Free Volume and the Mechanism of Plasticization in Water-Swollen Poly(vinyl alcohol). *Macromolecules* **1996**, *29*, 8137−8143.

(30) Zhang, Y.; Li, F.; Valenzuela, L. D.; Sammalkorpi, M.; Lutkenhaus, J. L. Effect of Water on the Thermal Transition Observed in Poly(allylamine hydrochloride)−Poly(acrylic acid) Complexes. *Macromolecules* **2016**, *49*, 7563−7570.

(31) Eneh, C. I.; Bolen, M. J.; Suarez-Martinez, P. C.; Bachmann, A. L.; Zimudzi, T. J.; Hickner, M. A.; Batys, P.; Sammalkorpi, M.; Lutkenhaus, J. L. Fourier transform infrared spectroscopy investigation of water microenvironments in polyelectrolyte multilayers at varying temperatures. *Soft Matter* **2020**, *16*, 2291−2300.

(32) Batys, P.; Zhang, Y.; Lutkenhaus, J. L.; Sammalkorpi, M. Hydration and Temperature Response of Water Mobility in

Poly(diallyldimethylammonium)−Poly(sodium 4-styrenesulfonate) Complexes. *Macromolecules* **2018**, *51*, 8268−8277.
(33) Koehler, R.; Steitz, R.; von Klitzing, R. About different types of water in swollen polyelectrolyte multilayers. *Adv. Colloid Interface Sci.* **2014**, *207*, 325−331.
(34) Scientific, B. *QCM-D Measurement*. https://www.biolinscientific.com/measurements/qcm-d (accessed Feb 1).
(35) Easley, A. D.; Ma, T.; Eneh, C. I.; Yun, J.; Thakur, R. M.; Lutkenhaus, J. L. A practical guide to quartz crystal microbalance with dissipation monitoring of thin polymer films. *J. Polym. Sci.* **2022**, *60*, 1090−1107.
(36) Reid, D. K.; Summers, A.; O'Neal, J.; Kavarthapu, A. V.; Lutkenhaus, J. L. Swelling and Thermal Transitions of Polyelectrolyte Multilayers in the Presence of Divalent Ions. *Macromolecules* **2016**, *49*, 5921−5930.
(37) Fares, H. M.; Wang, Q.; Yang, M.; Schlenoff, J. B. Swelling and Inflation in Polyelectrolyte Complexes. *Macromolecules* **2019**, *52*, 610−619.
(38) Iturri Ramos, J. J.; Stahl, S.; Richter, R. P.; Moya, S. E. Water Content and Buildup of Poly(diallyldimethylammonium chloride)/Poly(sodium 4-styrenesulfonate) and Poly(allylamine hydrochloride)/Poly(sodium 4-styrenesulfonate) Polyelectrolyte Multilayers Studied by an in Situ Combination of a Quartz Crystal Microbalance with Dissipation Monitoring and Spectroscopic Ellipsometry. *Macromolecules* **2010**, *43*, 9063−9070.
(39) Guzmán, E.; Ritacco, H.; Rubio, J. E. F.; Rubio, R. G.; Ortega, F. Salt-induced changes in the growth of polyelectrolyte layers of poly(diallyl-dimethylammonium chloride) and poly(4-styrene sulfonate of sodium). *Soft Matter* **2009**, *5*, 2130−2142.
(40) Nestler, P.; Paßvogel, M.; Helm, C. A. Influence of Polymer Molecular Weight on the Parabolic and Linear Growth Regime of PDADMAC/PSS Multilayers. *Macromolecules* **2013**, *46*, 5622−5629.
(41) Picart, C.; Mutterer, J.; Richert, L.; Luo, Y.; Prestwich, G. D.; Schaaf, P.; Voegel, J.-C.; Lavalle, P. Molecular basis for the explanation of the exponential growth of polyelectrolyte multilayers. *Proc. Natl. Acad. Sci.* **2002**, *99*, 12531−12535.
(42) Schlenoff, J. B.; Dubas, S. T. Mechanism of Polyelectrolyte Multilayer Growth: Charge Overcompensation and Distribution. *Macromolecules* **2001**, *34*, 592−598.
(43) Jukić, J.; Korade, K.; Milisav, A.-M.; Marion, I. D.; Kovačević, D. Ion-Specific and Solvent Effects on PDADMA−PSS Complexation and Multilayer Formation. *Colloids Interfaces* **2021**, *5*, 38.
(44) Ghostine, R. A.; Jisr, R. M.; Lehaf, A.; Schlenoff, J. B. Roughness and Salt Annealing in a Polyelectrolyte Multilayer. *Langmuir* **2013**, *29*, 11742−11750.
(45) Ghasemi, M.; Friedowitz, S.; Larson, R. G. Overcharging of polyelectrolyte complexes: an entropic phenomenon. *Soft Matter* **2020**, *16*, 10640−10656.
(46) Owusu-Nkwantabisah, S.; Gammana, M.; Tripp, C. P. Dynamics of Layer-by-Layer Growth of a Polyelectrolyte Multilayer Studied in Situ Using Attenuated Total Reflectance Infrared Spectroscopy. *Langmuir* **2014**, *30*, 11696−11703.
(47) Mähler, J.; Persson, I. A Study of the Hydration of the Alkali Metal Ions in Aqueous Solution. *Inorg. Chem.* **2012**, *51*, 425−438.
(48) Fu, J.; Fares, H. M.; Schlenoff, J. B. Ion-Pairing Strength in Polyelectrolyte Complexes. *Macromolecules* **2017**, *50*, 1066−1074.
(49) O'Neal, J. T.; Wilcox, K. G.; Zhang, Y.; George, I. M.; Lutkenhaus, J. L. Comparison of KBr and NaCl effects on the glass transition temperature of hydrated layer-by-layer assemblies. *J. Chem. Phys.* **2018**, *149*, 163317.
(50) Fares, H. M.; Ghoussoub, Y. E.; Surmaitis, R. L.; Schlenoff, J. B. Toward Ion-Free Polyelectrolyte Multilayers: Cyclic Salt Annealing. *Langmuir* **2015**, *31*, 5787−5795.
(51) Ghoussoub, Y. E.; Zerball, M.; Fares, H. M.; Ankner, J. F.; von Klitzing, R.; Schlenoff, J. B. Ion distribution in dry polyelectrolyte multilayers: a neutron reflectometry study. *Soft Matter* **2018**, *14*, 1699−1708.
(52) Lyu, X.; Peterson, A. M. The Princess and the Pea Effect: Influence of the first layer on polyelectrolyte multilayer assembly and properties. *J. Colloid Interface Sci.* **2017**, *502*, 165−171.
(53) Fares, H. M.; Ghoussoub, Y. E.; Delgado, J. D.; Fu, J.; Urban, V. S.; Schlenoff, J. B. Scattering Neutrons along the Polyelectrolyte Complex/Coacervate Continuum. *Macromolecules* **2018**, *51*, 4945−4955.
(54) Fares, H. M.; Schlenoff, J. B. Diffusion of Sites versus Polymers in Polyelectrolyte Complexes and Multilayers. *J. Am. Chem. Soc.* **2017**, *139*, 14656−14667.
(55) Dubas, S. T.; Schlenoff, J. B. Swelling and Smoothing of Polyelectrolyte Multilayers by Salt. *Langmuir* **2001**, *17*, 7725−7727.
(56) Reurink, D. M.; Willott, J. D.; Roesink, H. D. W.; de Vos, W. M. Role of Polycation and Cross-Linking in Polyelectrolyte Multilayer Membranes. *ACS Appl. Polym. Mater.* **2020**, *2*, 5278−5289.
(57) Hariri, H. H.; Lehaf, A. M.; Schlenoff, J. B. Mechanical Properties of Osmotically Stressed Polyelectrolyte Complexes and Multilayers: Water as a Plasticizer. *Macromolecules* **2012**, *45*, 9364−9372.
(58) Wende, C.; Schönhoff, M. Dynamics of Water in Polyelectrolyte Multilayers: Restricted Diffusion and Cross-Relaxation. *Langmuir* **2010**, *26*, 8352−8357.
(59) Chávez, F. V.; Schönhoff, M. Pore size distributions in polyelectrolyte multilayers determined by nuclear magnetic resonance cryoporometry. *J. Chem. Phys.* **2007**, *126*, 104705.
(60) Löhmann, O.; Zerball, M.; von Klitzing, R. Water Uptake of Polyelectrolyte Multilayers Including Water Condensation in Voids. *Langmuir* **2018**, *34*, 11518−11525.
(61) Batys, P.; Kivistö, S.; Lalwani, S. M.; Lutkenhaus, J. L.; Sammalkorpi, M. Comparing water-mediated hydrogen-bonding in different polyelectrolyte complexes. *Soft Matter* **2019**, *15*, 7823−7831.
(62) Ivanova, O.; Soltwedel, O.; Gopinadhan, M.; Köhler, R.; Steitz, R.; Helm, C. A. Immobile Light Water and Proton−Deuterium Exchange in Polyelectrolyte Multilayers. *Macromolecules* **2008**, *41*, 7179−7185.
(63) McCormick, M.; Smith, R. N.; Graf, R.; Barrett, C. J.; Reven, L.; Spiess, H. W. NMR Studies of the Effect of Adsorbed Water on Polyelectrolyte Multilayer Films in the Solid State. *Macromolecules* **2003**, *36*, 3616−3625.
(64) Smiatek, J. Theoretical and Computational Insight into Solvent and Specific Ion Effects for Polyelectrolytes: The Importance of Local Molecular Interactions. *Molecules* **2020**, *25*, 1661.
(65) Batys, P.; Luukkonen, S.; Sammalkorpi, M. Ability of the Poisson−Boltzmann equation to capture molecular dynamics predicted ion distribution around polyelectrolytes. *Phys. Chem. Chem. Phys.* **2017**, *19*, 24583−24593.
(66) Miller, M. D.; Bruening, M. L. Correlation of the Swelling and Permeability of Polyelectrolyte Multilayer Films. *Chem. Mater.* **2005**, *17*, 5375−5381.
(67) Lehaf, A. M.; Hariri, H. H.; Schlenoff, J. B. Homogeneity, Modulus, and Viscoelasticity of Polyelectrolyte Multilayers by Nanoindentation: Refining the Buildup Mechanism. *Langmuir* **2012**, *28*, 6348−6355.
(68) Farhat, T. R.; Schlenoff, J. B. Ion Transport and Equilibria in Polyelectrolyte Multilayers. *Langmuir* **2001**, *17*, 1184−1192.
(69) Kelly, K. D.; Fares, H. M.; Abou Shaheen, S.; Schlenoff, J. B. Intrinsic Properties of Polyelectrolyte Multilayer Membranes: Erasing the Memory of the Interface. *Langmuir* **2018**, *34*, 3874−3883.

https://doi.org/10.1021/acspolymersau.2c00008
ACS Polym. Au 2022, 2, 287−298